Research Article

Spatial variation of PGA using neural networks

Silvia R. García[1] · Miguel P. Romo[1] · Leonardo Alcántara[2]

Abstract
This work is oriented to studying the learning capabilities of neural networks and their impact on the development of a method for the generation of spatial variation of peak ground accelerations PGAs. This spatial variation is based on a limited number of accelerograms registered in specific geotechnical zones, along with a map of soil periods on the Mexico City area. The continuous surfaces that resulted are compared with the most common methods of interpolation, aiming to evidence the substantial advantages of NNs on those of these methods. Based on the results presented, it can be argued that using multi-parameters approaches to define spatial interpolations of a variable as important as PGA, allows to make safer engineering decisions.

Keywords Neural networks · Spatial predictive modelling · Spatial variation · Peak ground acceleration · Mexico City clay deposits · September 19th 2017 earthquake

1 Introduction

The design of a secure structure implies a good modelling of ground responses and this requires the most comprehensive compilation of information related to the soil's environment and the possible damages due to earthquakes [1]. Given the spacing and distribution between seismic monitors and geotechnical sampling sites, it is not always possible to obtain these data directly for each site under construction, so building codes usually offer parametric maps as guidelines for design of new works and reconstructions.

The challenge to geotechnical and earthquake engineering is to generate meaningful and reliable maps of spatial variability of soil properties and associated seismic responses [2, 3]. To solve this, engineers have turned to the use of available interpolation techniques due to the lack of certainty and the liability of costs when performing detailed geo-investigations [4–6]. The majority of the conventional interpolation schemes requires a relevant amount of input data to yield acceptable estimations. Because of these shortcomings it is necessary to search for new alternatives for developing spatial interpolation models.

In this research, a neural network NN [7] is presented as an alternative to analyze seismic and geotechnical parameters in a geographical context. The relations that exist between the spatial patterns of the stratigraphy and seismic responses beyond excessive physical simplifications are all contained in the spatial-neural model.

Other techniques such as Inverse Distance Weighting [8], Radial Basis Function [9], Local Polynomial [10] and Kriging [11], as well as the presented NN, are used to visualize the peak ground accelerations PGAs during the damaging September 19th 2017 earthquake that hit Mexico City. According to the results obtained, the best representation of PGAs contours can be conceived through the neural method, being the approximation that best locates the regions of maximum movements and higher levels

✉ Silvia R. García, sgab@pumas.iingen.unam.mx; Miguel P. Romo, mromo@pumas.iingen.unam.mx; Leonardo Alcántara, LAlcantaraN@iingen.unam.mx | [1]Geotechnical Engineering Department, Institute of Engineering, National University of Mexico, Ciudad Universitaria, Mexico City, Mexico. [2]Seismology Department, Institute of Engineering, National University of Mexico, Ciudad Universitaria, Mexico City, Mexico.

SN Applied Sciences (2019) 1:1381 | https://doi.org/10.1007/s42452-019-1269-7

Received: 14 January 2019 / Accepted: 11 September 2019 / Published online: 12 October 2019

of damages while unveiling its relationship with specific arrangements of materials.

In this document, in addition to this first introduction section, in Sect. 2 a brief presentation of the evolution of the interpolation methods is presented and the essential components of the alternative technique, neural networks, are listed. Without being exhaustive, this section tries to introduce the reader to the artificial intelligence tool, for those interested, references of great technical rigor are offered. Section 3 presents the application exercise, a spatial definition of the response (in terms of PGA) in Mexico City during three devastating earthquakes: September 19, 1985, October 9, 1995, and September 19, 2017. Neural networks predictions are compared with interpolation results from some techniques most commonly used in geotechnical-earthquake engineering to demonstrate the theoretical, conceptual and practical advantages of the artificial intelligence tool. The conclusions are presented in Sect. 4.

2 Spatial predictive modelling

A great expansion of the technical literature on the soil mapping through the use of different mathematical approaches, has been observed in the past decades. Some methods like linear and non-linear regression, geostatistics, and neural networks, among others, have been a recurrent implement for soil properties representation. A comprehensive review of computational methods used in digital mapping is presented by [12]; especially in the area of soil science. Park and Vlek [13] have analyzed the spatial variability of physical–chemical characteristics of soil, making use of NNs, regression trees and linear models. Other works with a detailed foundation are those of [14], in which satellite images plus GIS information and Bayesian methods have been applied, and also of [15] who in order to interpolate geologic layers borders used fuzzy neural networks. These scientists support the statement of the remarkable capacity of hybrid soft-computing methods to successfully perform these tasks [16–18].

For the approximation of the values of a variable at locations that have not been sampled, the procedures, in the context of Earth Sciences, involve well-known interpolation techniques like linear regression, ordinary kriging and co-kriging [19–22]. Regionalized variable theory has been used to estimate soil data providing a summary of soil variability in the form of a semi-variogram and a predictive technique, kriging, for unobserved values [23, 24]. This technique has become the most worked in scientific environments in which it is required to interpolate values of properties at low cost, however the information requirements grow as the size of the area that is analyzed increases.

The application of NN (the artificial intelligence tool that mimics the human brain processes) in spatial data analysis can be divided into two major categories: (1) remote sensing, and (2) spatial modelling [25, 26]. Some successful examples on spatial modeling using NNs [27, 28], fuzzy logic [29, 30] and genetic learning [14] have contributed to the demonstration that the utilization of artificial intelligence tools leads significantly to the development of important geological and geotechnical topics.

2.1 General comments on neural networks

Neural networks NNs have been positioned in the last decades, as relevant instruments especially for complex processes modeling. This technique demonstrates to be particularly suitable when the development of phenomenological or conventional regression models results unmanageable. NNs represents an approach which resorts computer modeling to learn from examples without demanding of previous knowledge of the relationships among parameters; the iterative learning process permits to NNs adapt themselves to changing, uncertain, noisy environments.

The NN-based models constructed from historic process input–output data, display excellent generalization abilities that permit to have accuracy in the predictions for new input data sets. Additionally, multiple input-multiple output nonlinear relationships can be simultaneously and easily approximated.

In order to cope with the input–output duality problem, the NN paradigm that professionals resort to the most of times is the multilayered perceptron, MLP. An approximation or mapping of any nonlinear computable function to an arbitrary degree of accuracy, can be elaborated by means of a three-layered MLP with a single intermediate (hidden) layer. To have an accurate execution of the simulations there should be a sufficiently large number of nodes, known as hidden neurons or processing elements. The physics encrypted in the input–output database is discovered by the NN through the learning process. Through the use of an iterative numerical procedure along with any of the training algorithms that have been published elsewhere (i.e., [7, 31–33]), is that this task can be achieved.

In Fig. 1 the architecture of the MLP that was used in this work is shown. The neural structure is formed by input, hidden and output layers that are respectively represented with N, L and K letters. The total of nodes of a given layer are connected by means of links, or weights, to all nodes of the next layer that is moving forwardly once the output layer has been reached. A bias node (with fixed output of + 1) is included in the MLP that means supplementary

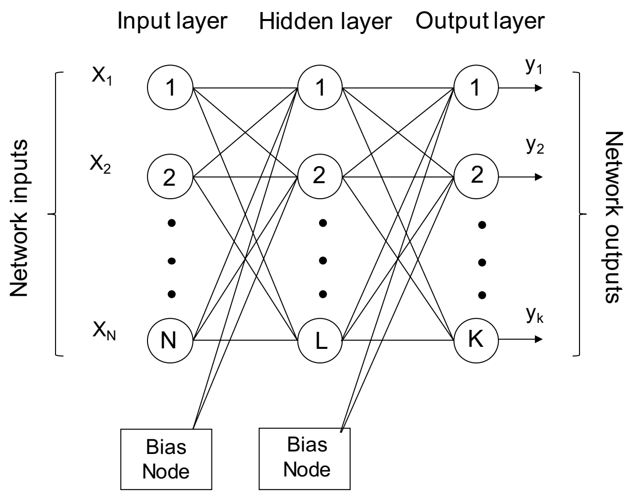

Fig. 1 Architecture of the MLP used in this study

adjustable parameters (weights) for the fitting of the model. The inputs and the number of nodes N need to be equal and the number of processed outputs determines the number of nodes K. Nevertheless, the number of hidden nodes L is associated with the problem or NN task and with the desired approximation and generalization capabilities of the network model. The success of the learning process of a NN can be considered as long as the system displays good prediction on unknown test data.

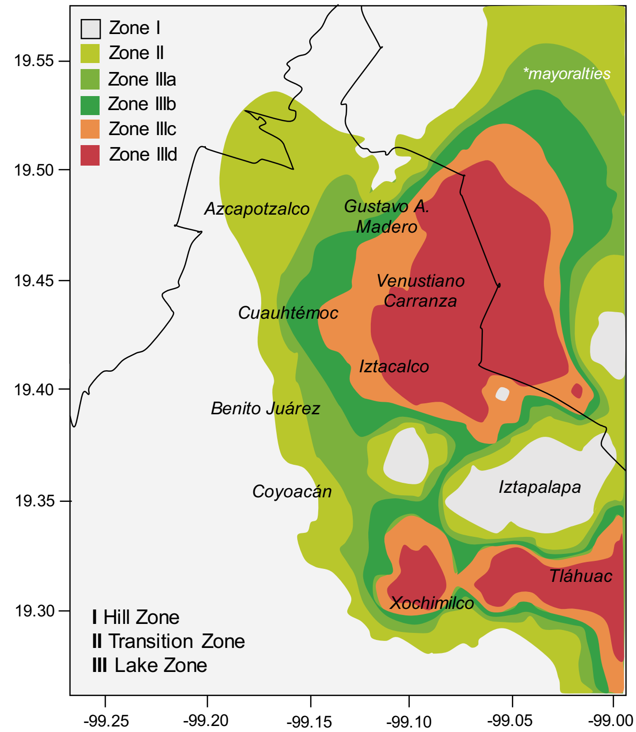

Fig. 2 Geotechnical Zonation for Mexico City (modified from GDFb, 2004)

3 Neuro-spatial estimation of PGA

The modelling of the spatial variation of PGAs during some earthquakes that have struck Mexico City, was developed. The main objective was to define the variations between geotechnical zones because, in seismic design of structures, recognizing the spatial variation of the earthquake force dependent of the soils deposits is a crucial step. Using strong motion recordings from accelerometer arrays at the area, the NN is constructed and validated.

3.1 Data base and topology of the network

The Mexico Basin holds the metropolitan area and contains the remnants of the Chalco and Texcoco lakes. The drying process of the bodies of water and the deposition mechanisms gave rise to sequences of materials that are dependent of the position on the antique lakes systems. In the center of the city, for (Texcoco lake) a superficial *Dry Crust* (DC), a *First Clay Layer* (FCL) of several tens of meters thick, a *First Hard Layer* (FHL), a *Second Clay Layer* (SCL) and the so-called *Deep Deposits* (DD) can be found [34]. This arrangement changes as it approaches the mountains, it

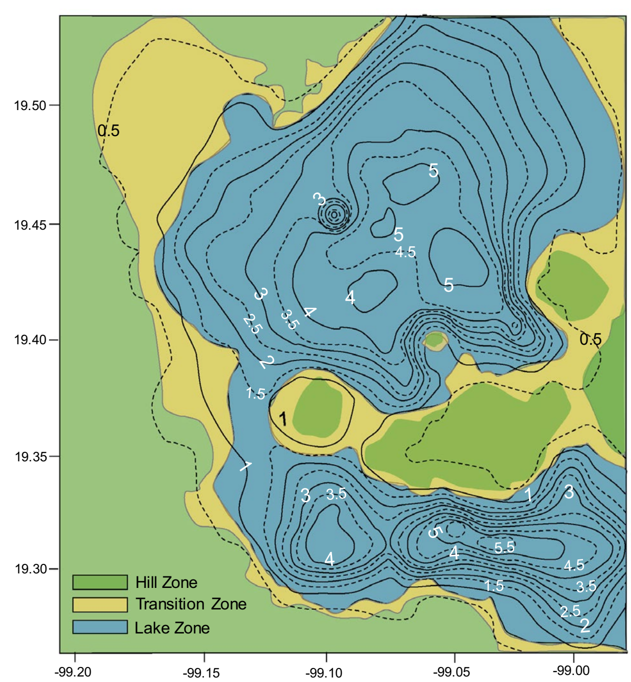

Fig. 3 Microzoning map of isoperiod curves (modified from Avilés et al. 2006)

Table 1 Parameters of the tried architectures

ID	Number of hidden layers	Number of hidden neurons per layer	Number of iterations	Number of training samples	Number of testing samples
85-A	1	50	850	9	2
85-B	2	50	320	9	2
85-C	1	150	725	9	2
95-A	2	50	920	26	8
95-B	1	100	1430	26	8
95-C	1	150	2205	26	8
17-A	1	500	4010	38	10
17-B	2	50	1960	38	10
17-C	2	100	3420	38	10

Table 2 Average accuracy and standard deviation of the three Architectures for different values of iterations keeping constant the learning rate

	5500 iterations	10,000 iterations
1 Hidden layer 50 nodes	97.2 ± 0.22%	98.7 ± 0.19%
2 Hidden layers 50 nodes/layer	96.1 ± 0.31%	99.0 ± 0.12%
1 Hidden layer 150 nodes	94.7 ± 0.52%	93.1 ± 0.78%

Station	ActualValue	Predicted Value	Absolute error	Relative error
TACY	33.97	28.9	-1.13	0.03326
CDAO	84.61	82.1	2.51	0.02967

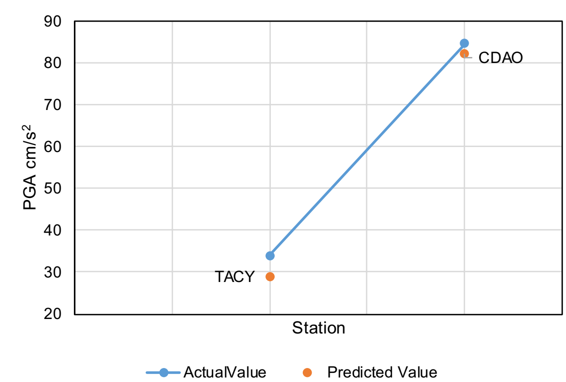

Fig. 4 Predicted and actual values for testing samples, the Sept 19th 1985 event

can even change very drastically between sites separated by a few meters on the surface.

Based on information processed from hundreds of soundings, Mexico city's building code [35–37] recommended a division of the subsoil of the metropolis in three geotechnical zones (Fig. 2): *Zone I-Hills*, formed by hard soils- rock like deposits firm deposits, *Zone II-Transition*, constituted by erratic intercalations (in size and arrangement) of loose sands and clays with heterogeneous moisture contents, and *Zone III-Lake* that consists of clay sediments of with high water content and high compressibility.

Based on the catastrophic experiences related to the 1985 seismic event that hit the Mexico City, the building codes were corrected to take into account the impressive energy content that could be generated from the Mexican Pacific [38] and, until then, different ways of responding from the soils.

With spectral amplification functions for about 100 instrumented soft sites at Mexico City [39], complemented with around 500 microtremor measurements, predominant ground periods Ts have been studied and calculated for a grid of 80 × 80 points covering most part of the city [40]. This resulted in the microzoning map displayed in Fig. 3. The isoperiod curves for Ts = 0.5 and 1 s roughly mark the separations between both the firm and transition zones as well as the transition and soft zones, respectively.

In addition to parameters that describe the environment, to model the spatial variation of PGA, it is necessary to situate the seismic monitors. The Accelerographic Network for Mexico City, RACM (abbreviations in Spanish) is constituted by more than 80 accelerographs distributed in the surface, in buildings and underground. This number of stations have been growing from the disastrous earthquakes of 1985. The accelerographs used in this investigation are installed in the different zones in the valley of Mexico that means, firm ground, intermediate ground and soft ground.

The previously described geotechnical zonation, the predominant ground periods Ts and the location (Latitude, Longitude) of the accelerographic stations are the information used as inputs of the NN. In the neuro spatial analysis, the function PGA = *f* {(Lat, Long, Geotechnical Zone, Ts)} is to be approximated, with which the PGA values at any surface point can be determined.

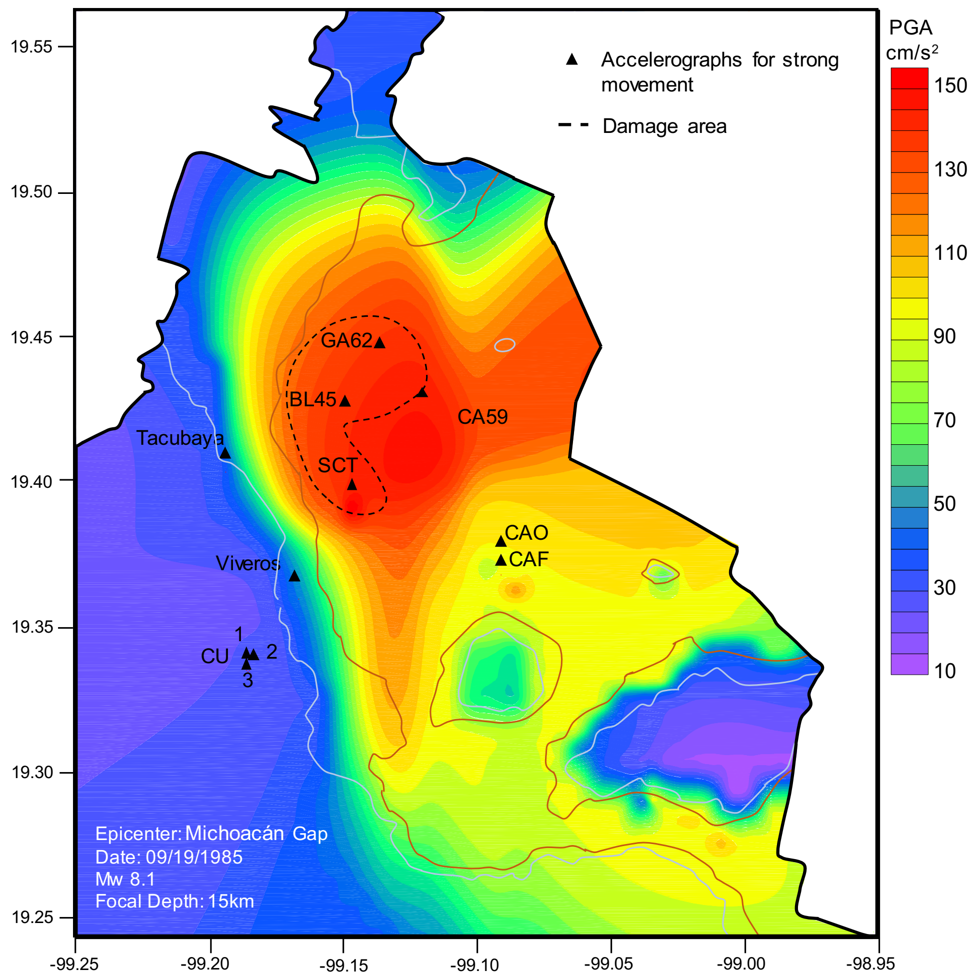

Fig. 5 PGA Neural distribution for the 1985 Michoacán Earthquake

The 80% of the stations were used to construct the network and the remaining 20% is separated for validation of the model. In addition to checking that the values estimated by the network are below the error declared as objective, the congruence of the PGA contours is verified.

It is important to point out that the proposed NN is not used here merely as a spatial interpolator for estimating the PGA values at unobserved locations. The neural tool is a spatial method that captures spatial dependency in a kind of multidimensional and multiparametric regression analysis, providing useful information on 2D relationships among the soils, topography and PGAs involved.

3.2 Neuro-contours of PGAs

The ground motions registered during the iconic 1985, September 19th, Michoacán Earthquake, (Mw 8.1), a medium intensity event (Mw 7.6) and the most recent devastating shaking, the 2017 September 19th (Mw 7.1), Morelos-Puebla event are used as examples of the neural methodology results.

Station	ActualValue	Predicted Value	Absolute error	Relative error
BL45	13.54	12.99	0.55	0.04062
CJ03	15.04	14.6	0.44	0.02926
HA41	11.44	7.08	2.36	0.20629
TL55	7.65	7.01	0.64	0.08366
VM29	17.28	14.3	2.98	0.17245
CP28	1.72	0.7	1.02	0.59302
ESTS	1.13	2.5	-1.37	1.21239
TACY	2.2	2.7	-0.5	0.22727

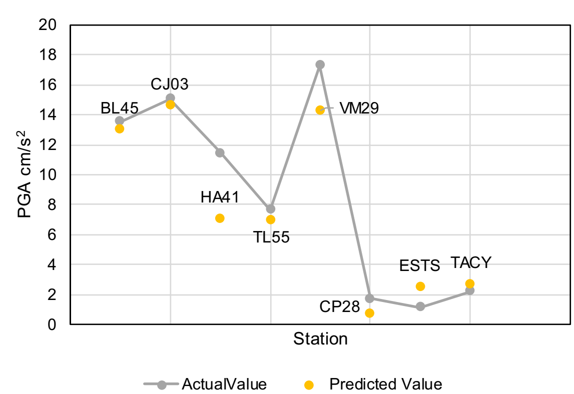

Fig. 6 Predicted and actual values for testing samples, the Oct 9th 1995 event

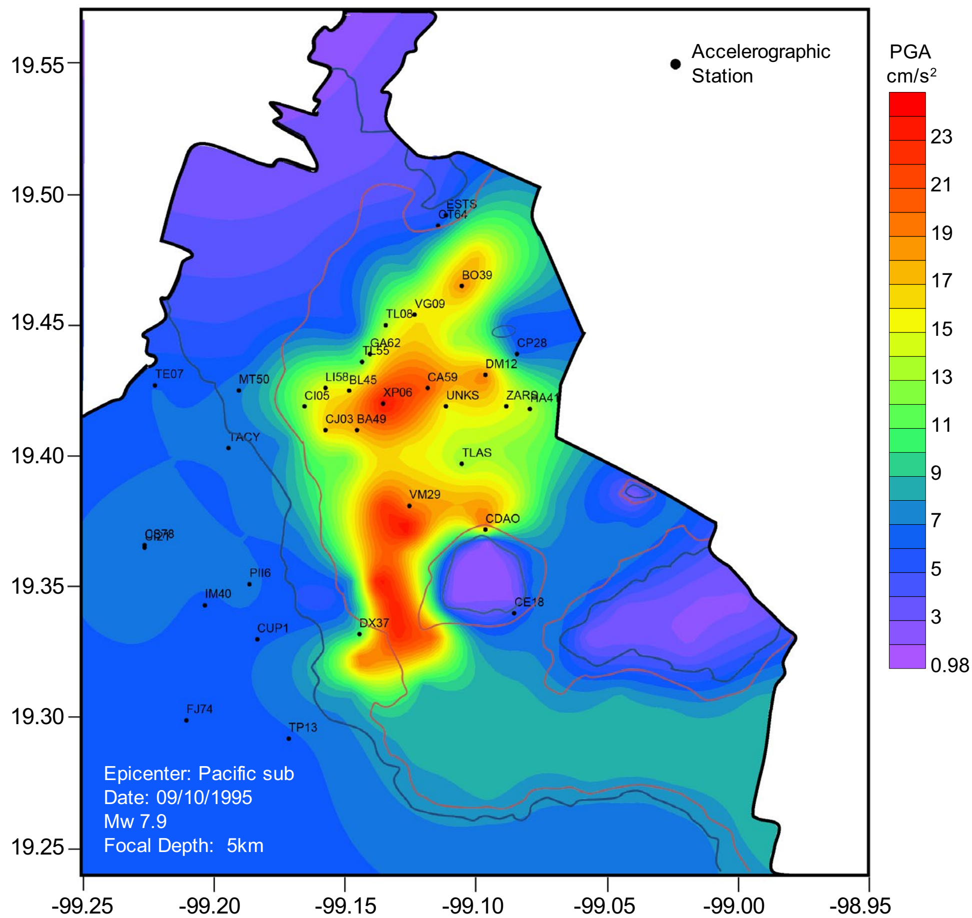

Fig. 7 The neuro-PGAs distribution during the October 9th 1995 (Mw 7.9) event

For this model, Back Propagation algorithm [41, 42] was selected and the momentum gradient descent method as the network training method. The momentum factor has been set to 0.8, the learning rate to 0.05, the maximum number of the training times to 10,000, and the expected error is 1.0 (in cm/s^2). The model convergence calculation uses the mean square error (MSE) function as the optimization objective function:

$$E = \frac{1}{N}\sum_{i=1}^{N}\left(y_i^d - y_i\right)^2$$

where E is MSE, N is the number of samples, y_i^d is the ideal output, y_i is the actual output. The network converges until the network global error E is less than expected error.

The PGA-model structure uses a three layers neural network which includes an input layer IL, one or two hidden layers HL, and an output layer OL. The structure is IL-HL-OL. The input layer contains four neurons corresponding to the geotechnical (zonation) and seismological (fundamental period Ts) parameters coupled with the position (Latitude, Longitude) of the stations. The output layer has one neuron (the PGA). The hidden layer transfer function is sigmoid while the output layer transfer function is purelin. In Table 1 the parameters of the tried architectures are shown.

The criterion to select the architecture that best meets the objective of predicting PGA, one indispensable condition must be reached: that the NN to through the training process present the best compromise be-tween precision and generality. Because of the number of monitors existing, the amount of data available to estimate PGA at each point on the surface is very limited. So in order to avoid overfitting a cross-validation approach was used to search for the optimal model. To define the predictive accuracy of the set of neural architectures an independent set of data (test samples) were used. With the k-fold cross-validation the samples for each seismic event were randomly partitioned into k sets (k = 5). Once the errors across the different test sets were calculated for each NN, they were compared and the architecture with the lowest values was labeled as the optimal model.

Station	ActualValue	Predicted Value	Absolute error	Relative error
FJ74	91.0565	90.18	0.8765	0.00963
EO30	82.1321	82.49	-0.3579	0.00436
MT50	58.2667	76.8	0.3767	0.00647
CO56	113.992	132	-7.008	0.06148
NZ31	97.7278	78.9	1.2278	0.01256
JA43	106.286	103.5	2.786	0.02621
SI53	177.565	170.35	7.215	0.04063
BO39	95.1432	99.55	-4.4068	0.04632
CE23	59.9871	62.02	-2.0329	0.03389
DM12	90.5161	83	0.5061	0.00559

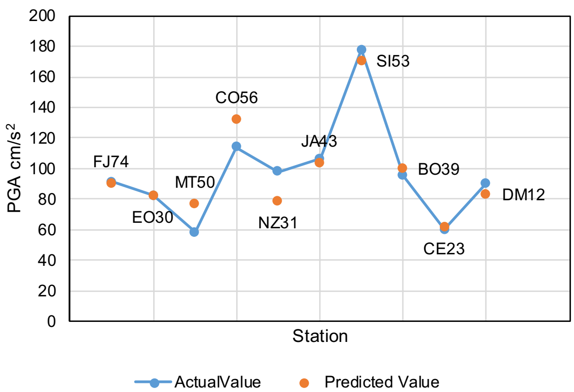

Fig. 8 Predicted and actual values for testing samples, the Sept 19th 2017 event

September 19th 1985 During the Michoacán earthquake (Mw8.1) only eleven recording stations were in operation, three in the hilly area and the rest in the lake and transition zones. From these sites two acceleration stations were selected to test the network and the rest were left for training the NNs. In Table 2 the results obtained for the 3 best network architectures are shown. After tried with different architectures and based on the k-cross validation results, the 4-50-50-1 model was considered the optimal. The comparison of the predicted and actual values for the training and test validation samples is shown in Fig. 4. It can be seen that the errors of the accelerations predictions are sufficiently low from the point of view of engineering practice.

Then, this NN was used to predict the PGAs on a mesh (grid every 150 m) on the surface of Mexico City (included inside the thick continuous line) and their spatial display is shown in Fig. 5.

Severe damages occurred in the metropolis, despite of the distance of 300 km to the rupture area. The scale of the destruction was mainly attributed to the dynamic amplification of the lakebed deposits (in Fig. 4, the area of maximum damage is within the dashed line). It is remarkable that the neural pattern of PGAs-distribution is very congruent with the areas that have outstanding amplification potential (Lake Zone with particular Ts-isocurves) and highest number of collapses. Besides the acceptable correlation between measured and estimated PGAs, the distribution of acceleration levels is adequately anticipated for each geotechnical zone.

October 9th 1995 The Tecomán earthquake (Mw7.6) struck the area near the town of Manzanillo, Colima, affecting the southwestern part of Jalisco (on the coast of the Mexican Pacific). Around the epicentral area more than 17,000 structures suffered significant damage (3000 of them collapsed), affecting cities or municipalities with nearly 45,000 inhabitants. Unfortunately, 60 deaths were recorded in different states near the epicenter. In Mexico City, about 540 km from the epicentral zone, this earthquake felt strongly and caused alarm in the population, even activated the protocols for post-seismic reviews.

Over the years and after the painful experience of 1985, the efforts to implement useful instrumentation in the areas with the greatest potential for amplification, led to the start-up of many more registration stations. Using the information from 34 stations (separating eight stations to test the network) the neuro-PGAs distribution during the Tecomán event was developed. Following the procedure described for the 1985 event, many possible architectures were tried and the 4-150-1 arrangement was finally considered the best. The error between the registered and the predicted PGAs is very low (Fig. 6). Again, the NN is applied to predict the PGAs on a smaller mesh (grid every 100 m) on the surface of Mexico City and their spatial display is shown in Fig. 7.

As can be seen, as more stations are involved the zones of uppermost amplitudes are better defined. The spatial variation of the ground accelerations is complex and its connection with the thickness of the clay deposits starts to be clearer. However, the southern transition zone is still a region with poor spatial definition.

September 19th 2017 The intermediate-depth normal-fault earthquake occurred approximately 120 km away from Mexico City (Mw 7.1), produced the collapse of more than 50 structures in the capital city, which resulted in more than 330 deaths. This has been the most intense earthquake to hit Mexico City since the Michoacán event. Preliminary studies of the characteristics of collapsed buildings shown that the losses were primarily located in Zones IIIa and IIIb (subdivisions of Lake Zone) of the microzonation of the building code, regions with total thickness of soft clay deposits between 25 and 40 m and by predominant periods of vibration between 1 s and 2 s.

With 48 stations registering the movement, a valuable set of PGAs could be related to a broad range of fundamental periods and stratigraphies. From these sites 10 acceleration stations were selected to test the network and the rest were left for training. Between the many different

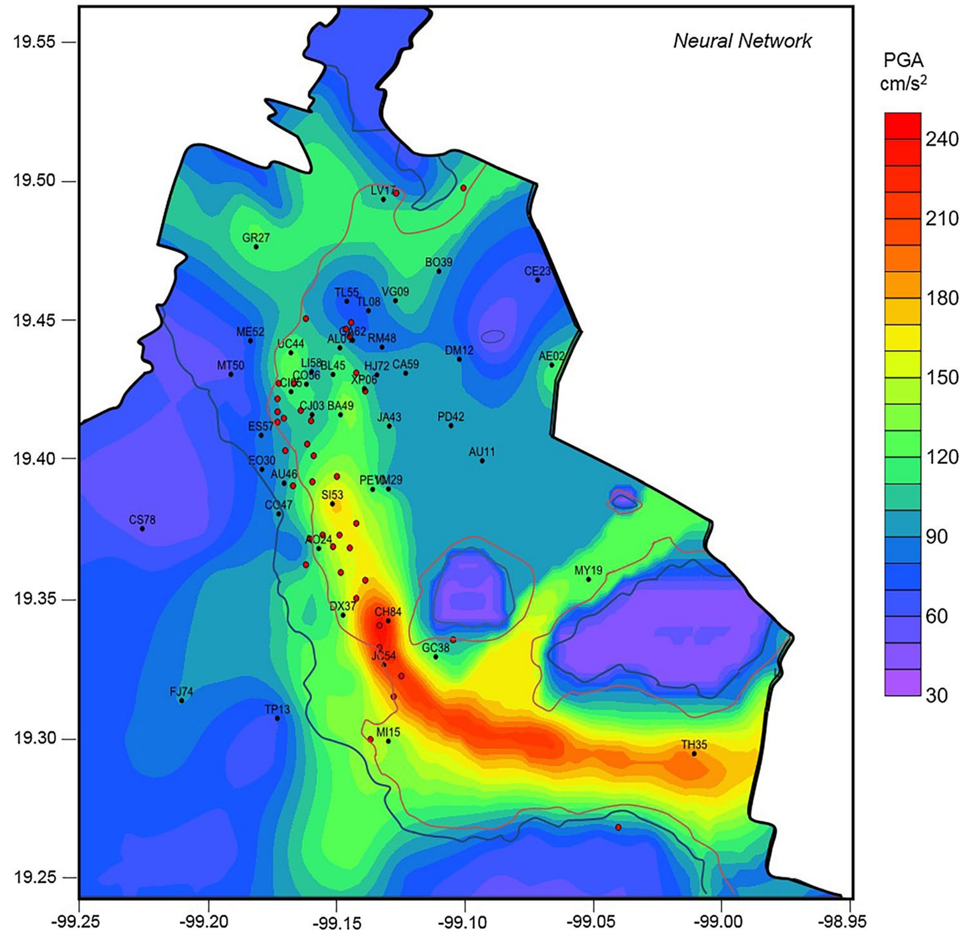

Fig. 9 Distributions calculated from Neural Network

architectures tried the 4-100-100-1 structure was considered the optimal. The predicted and actual values of PGAs, for the training and test validation samples, are very closer (Fig. 8). This neural model was used to construct the 2D variation, shown in Fig. 9 (on a grid every 50 m). The remarkable capacity of the NN for predicting the PGAs in the three different geotechnical zones can be seen. The collapsed buildings are concentrated around 120-240 cm/s^2 (Zones IIIa and IIIb, right on the border with the Transition Zone) but the highest levels of PGAs were generated in a not completely-defined geotechnical zone with evidence of considerable topographic effects.

After an earthquake like the one in 2017, with the damages and human casualties recorded, it is very important to know the PGAs that were reached at every point of the metropolis (potential sites to develop constructions). For this purpose, normally interpolation methods such as those shown in the Fig. 10 are used. The techniques assessed include deterministic and stochastic methods (Inverse Distance Weighting, Radial Basis Function, Local Polynomial and Kriging). Selecting the appropriate method is fundamental so it is very important to point out the differences between the distributions calculated from the different schemes. In Table 3 the values of accelerations measured in six stations are compared with those obtained from the contours derived from each method. It is important to note that these cases were used to develop the variations of the deterministic and stochastic methods, but they were not included to construct the NN model so they are "blind" cases.

In addition, the only tool capable of recognizing the natural obstacles (mountainous units) and the geotechnical zoning is the NN. The neural contours even show an important variation in the Hill Zone, which is in agreement with the recognized differences between materials in the region (i.e. rock, rock-like, stiff materials). The definition of the differences between Transition and Lake is very remarkable when compared with the spatial determinations derived from the traditional methods. The definition of the differences in the transition is very remarkable

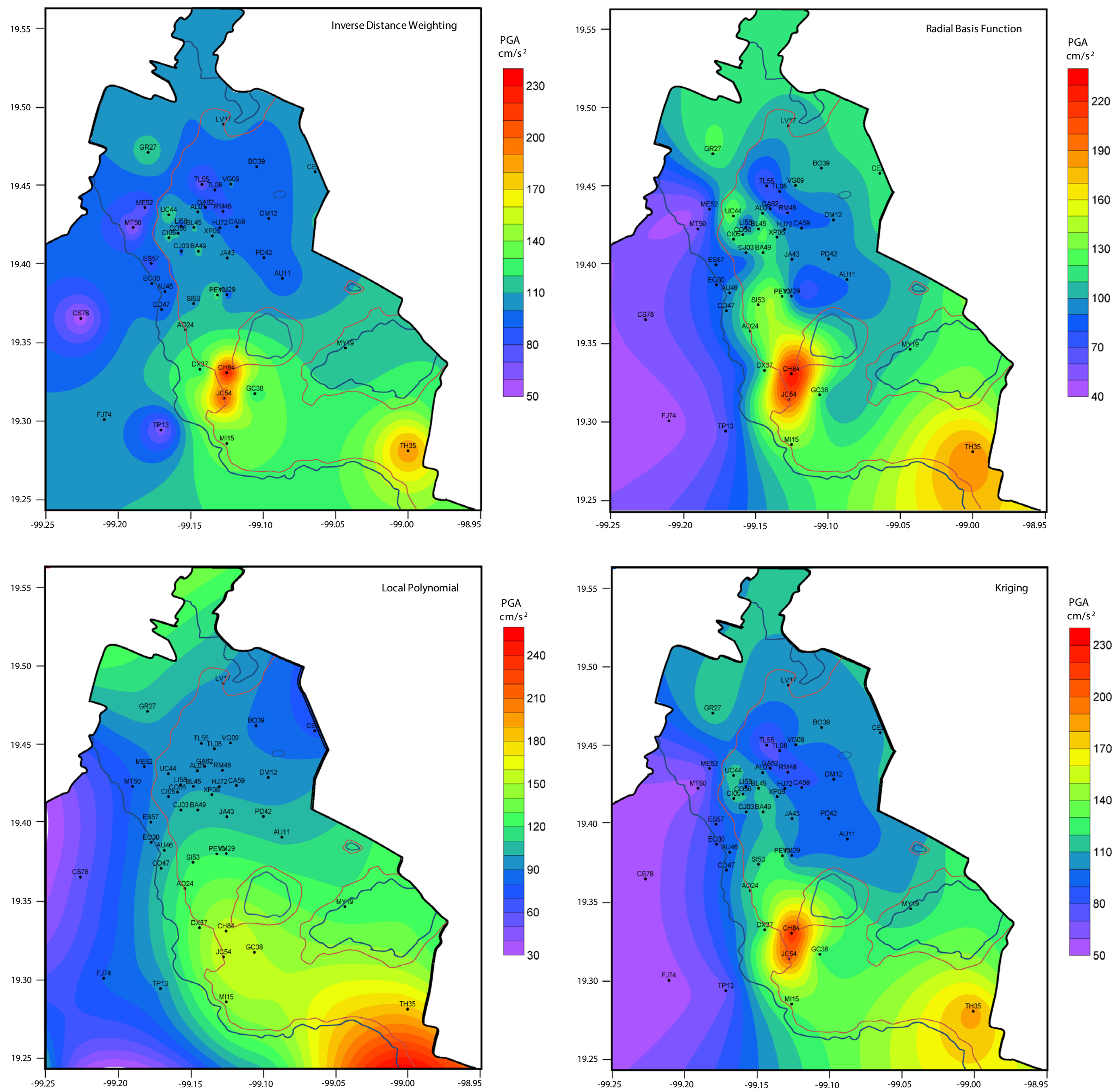

Fig. 10 Distributions calculated from different methods of interpolation

Table 3 Values of accelerations measured during the September 19th 2017 earthquake in six stations compared with those obtained from the contours derived from each method, for the NN these stations were test cases

Station	Acceleration registered	Neural network	Inverse distance	Radial basis	Local polynomial	Kriging
Peak ground acceleration						
EO30	82.1321	82.49	95.94	85.49	93.89	86.1
FJ74	91.0565	90.18	103.82	47.83	79.84	56.92
JA43	106.286	103.5	102.01	98.11	106.29	102.6
SI53	177.565	170.35	108.65	133.41	120.29	117.67
BO39	95.1432	99.55	97.33	107.62	89.11	102.72
CE23	59.9871	62.02	102.72	113.07	77.03	109.52

when compared with the spatial determinations derived from the traditional methods. This is very important when dealing with zoning for building codes because the area responds to seismic inputs in a chaotic or undeterministic manner, the display with the conventional methods could minimize or oversimplify this fact.

4 Conclusions

Conventional interpolating estimators require a great number of measurements accessible, what is generally impractical. In this investigation, NNs are presented as a flexible, efficient and convenient multiparametric-tool for the interpretation of geotechnical and seismological information for modelling the spatial variation of PGAs. The neural technique can be used to integrate systematically the results of soil monitoring and exploration, handling the inherent in situ testing uncertainty and taking advantage of broad stratigraphic descriptions. The presented results prove that NNs are able to better define the shape of accelerations contours that are limited by natural accidents and the complex characteristics of soil deposits.

Between the advantages of using NNs in the spatial interpolation of this important seismic variable we can mention:

- Able to recognize very complex relationships between incoming seismic shocks and the reaction pattern of specific soil columns.
- The NN is straightforward to use and to implement in practice. Having reliable accelerations predictions in regions where seismic monitors are not available is by far the most attractive aspect of this neural model.
- Compared with the other interpolation techniques, the NN is relatively tolerant to noisy cases with remarkable good predictive capabilities
- The integration of the neural model and their results in a GIS is absolute.

While some of the disadvantages that the authors have been able to recognize are:

- It is still evident that the NN needs as many training cases as possible.
- For phenomena such as seismic in which the absence of data is a constant, overfitting is a very high risk, being higher the smaller the test set.
- Derived from its black box nature, the interpretation of the internal behavior of the network is very difficult and this is a limitation to achieve acceptance among professionals involved in the subject.

Complaince with ethical standards

Conflict of interest The authors declare that they have no conflict of interest.

References

1. Patel A (2019) Geotechnical investigations and improvement of ground conditions. Woodhead Publishing Series in Civil and Structural Engineering, p 209
2. Aspasia Zerva and Vassilios Zervas (2002) Spatial variation of seismic ground motions: an overview. Appl Mech Rev 55(3):271–296. https://doi.org/10.1115/1.1458013
3. Assimaki Dominic, Pecker Alain, Popescu Radu, Prevost Jean (2003) Effects of spatial variability of soil properties on surface ground motion. J Earthq Eng. https://doi.org/10.1080/13632460309350472
4. Mzuku M, Khosla R, Reich R, Inman D, Smith F, MacDonald L (2005) Spatial variability of measured soil properties across site-specific management zones. Soil Sci Soc Am J 69(5):1572–1579. https://doi.org/10.2136/sssaj2005.0062
5. Shit PK, Bhunia GS, Maiti R (2016) Spatial analysis of soil properties using GIS based geostatistics models. Model Earth Syst Environ 2:107
6. Lin H, Wheeler D, Bell J, Wilding L (2005) Assessment of soil spatial variability at multiple scales. Ecol Model 182:271–290
7. Haykin S (2008) Neural networks and learning machines. Pearson Prentice Hall, New Jersey
8. Wong (2017) Interpolation: inverse-distance weighting. In: International encyclopedia of geography: people, the earth, environment and technology, Wiley Online Library
9. Buchmann (2003) Radial basis functions: theory and implementations. Cambridge University Press, Cambridge
10. Fox J, Sanford W (2011) Nonparametric regression in R: an appendix to an R companion to applied regression, 2nd edn. SAGE Publications, Inc. ISBN-13: 978-1412975148
11. David (1988) Handbook of applied advanced geostatistical ore reserve estimation. Elsevier Science Publ. Co., New York
12. McBratney AB, Mendonca Santos ML, Minasny B (2003) On digital soil mapping. Geoderma 117:3–52. https://doi.org/10.1016/S0016-7061(03)00223-4
13. Park SJ, Vlek PLG (2002) Environmental correlation of three-dimensional soil spatial variability: a comparison of three adaptive techniques. Geoderma 109(1–2):117–140. https://doi.org/10.1016/S0016-7061(02)00146-5
14. Zhou J, Civco D (1996) Using genetic learning neural networks for spatial decision making in GIS. Photogramm Eng Remote Sens 62(11):1287–1295
15. Kumar JK, Konno Masao, Yasuda Noboru (2000) Subsurface soil-geology interpolation using fuzzy neural network. J Geotech Geoenviron Eng 126(7):632–639. https://doi.org/10.1061/(ASCE)1090-0241(2000)126:7(632)
16. Shahin MA, Mark B, Holger R (2001) Artificial neural network applications in geotechnical engineering. Aust Geomech J 36(1):49–62
17. Parente CL, Araújo ME, Araújo J (2007) Diversity of cetaceans as tool in monitoring environmental impacts of seismic surveys. Biota Neotrop 7(1):49–55. https://doi.org/10.1590/S1676-06032007000100007
18. Samui P, Das S, Sitharam TG (2010) Soft computing: in geotechnical engineering. VDM Verlag, Germany

19. Leenaers H, Okx JP, Burrough PA (1990) Comparison of spatial prediction methods for mapping floodplain soil pollution. CATENA 17(6):535–550. https://doi.org/10.1016/0341-8162(90)90028-C
20. Voltz M, Webster R (1990) A comparison of kriging, cubic splines and classification for predicting soil properties from sample information. Eur J Soil Sci 41(3):473–490. https://doi.org/10.1111/j.1365-2389.1990.tb00080.x
21. Kollias VJ, Kalivas DP, Yassoglou NJ (1999) Mapping the soil resources of a recent alluvial plain in Greece using fuzzy sets in a GIS environment. Eur J Soil Sci 50:261–273. https://doi.org/10.1046/j.1365-2389.1999.t01-1-00231.x
22. Chambers R, Hird K, Yarus J (2000) Petroleum geostatistics for nongeostaticians. Geophys Lead Edge Explor 19(6):592–599. https://doi.org/10.1190/1.1438630
23. Journel AG, Huijbregts, Ch J (1978) Mining geostatistics. The Blackburn Press, New York
24. Matheron G (1973) The intrinsic random functions and their applications. Adv Appl Probab 5(03):439–468. https://doi.org/10.2307/1425829
25. Gong P (1994) Integrated analysis of spatial data from multiple sources: an overview. Can J Remote Sens 20:349–359. https://doi.org/10.1080/07038992.1994.10874578
26. Sui DZ (1994) GIS and urban studies: positivism, post-positivism and beyond. Urban Geography 15:258–278. https://doi.org/10.2747/0272-3638.15.3.258
27. Wang FJ (1992) Incorporating a neural network into GIs for agricultural land suitability analysis. GIS/LIS 192(1):804–815
28. Deadman P, Gimblett R (1997) Applying neural networks to vegetation management plan development. AI Appl 11(3):107–112
29. Sui DZ (1993) Integrating neural networks with GIS for spatial decision making. Oper Geogr 11:13–20
30. Sui DZ (1994) Fuzzy logic can help GIS cope with reality. GIS World, Fort Collins, Colorado
31. Riedmiller M, Braun H (1993) A direct adaptive method for faster backpropagation learning: the RPROP algorithm. IEEE Int Conf Neural Netw 1:586–591. https://doi.org/10.1109/ICNN.1993.298623
32. Zurada J, Liu W, Wang L (2006) Chaotic cellular neural networks with negative self-feedback. In: Proceedings of the eight international conference on artificial intelligence and soft computing, vol 1, Zakopane, Poland, pp 66–75. https://doi.org/10.1007/11785231_8
33. Benuskova L, Kasabov N (2007) Computational neurogenetic modeling. Springer, New York. https://doi.org/10.1007/978-0-387-48355-9
34. Gobierno del Distrito Federal (GDFa) (2004) Reglamento de construcciones para el Distrito Federal. Official Gazette of Distrito Federal, México
35. Gobierno del Distrito Federal (GDFa) (2004) Normas Técnicas Complementarias para Diseño y Construcción de Cimentaciones para el Distrito Federal. Official Gazette of Distrito Federal, México
36. Marsal R, Mazari M (1959) El subsuelo de la Ciudad de México. Facultad de Ingeniería I y II, UNAM, Mexico
37. Auvinet (2016) Geotechnical Zoning of Mexico Valley Subsoil. Ingeniería Investigación y Tecnología 17(3):297–308
38. Ordaz M, Krishna Singh S (1992) Source spectra and spectral attenuation of seismic waves from Mexican earthquakes, and evidence of amplification in the hill zone of Mexico City. Bull Seismol Soc Am 82(1):24–43
39. Avilés J, Pérez-Rocha LE, Aguilar HR (2006) Influence of ground water extraction in the seismic hazard of Mexico City. WIT Trans Ecol Environ. https://doi.org/10.2495/GEO060451
40. Pérez-Rocha LE, Ordáz M, Sánchez-Sesma FJ (1995) Spatial interpolation of seismic data: the case of the Valley of Mexico. In: Proceedings of the 10th Pan-American conference on soil mechanics and foundation engineering, Guadalajara, Mexico
41. Werbos (1982) Applications of advances in nonlinear sensitivity analysis. In: System modeling and optimization. Springer, Berlin, pp 762–770
42. Rumelhart David E, Hinton Geoffrey E, Williams Ronald J (1986) Learning representations by back-propagating errors. Nature 323(6088):533–536